

## Formation of jarosite and its effect on important ions for *Acidithiobacillus ferrooxidans* bacteria

B. NAZARI<sup>1</sup>, E. JORJANI<sup>1</sup>, H. HANI<sup>1</sup>, Z. MANAFI<sup>2</sup>, A. RIAHI<sup>2</sup>

1. Department of Mining Engineering, Tehran Science and Research Branch, Islamic Azad University, Tehran, Iran;

2. Hydrometallurgy Research Center, Sarcheshmeh Copper Complex,  
National Iranian Copper Industries Company, Iran

Received 13 June 2013; accepted 5 February 2014

**Abstract:** The precipitation of jarosite adversely affects the bio-leaching of copper sulfides in the Sarcheshmeh heap bio-leaching process. The variables of the initial concentration of ferrous iron in the growth medium, pH, and temperature were examined in the laboratory to determine how they affect the precipitation of jarosite in the presence of *Acidithiobacillus ferrooxidans* bacteria. It was found that the maximum ferric precipitate occurred at a ferrous sulfate concentration of 50 g/L, a temperature of 32 °C, and an initial pH value of 2.2. The effects of the precipitation of ferric iron on the quantities of ions that are important for *A. ferrooxidans* bacteria in aqueous phase, i.e., ferric, sulfate, potassium, phosphate, and magnesium ions, also were assessed. The results showed relatively similar patterns for the ferric and potassium ions, and then reason might have been the co-precipitation of these ions as constituent elements of jarosite mineral. At pH values greater than 1.6, the solubility of phosphate ions decreased dramatically due to the co-precipitation of phosphate ions with the jarosite precipitate and due to the significant growth rate of *A. ferrooxidans* bacteria in this pH range. Due to the dissolution of a gangue constituent in the ore, the magnesium levels increased in the first few days of the bio-leaching process; thereafter, it decreased slightly.

**Key words:** jarosite formation; copper bio-leaching; *Acidithiobacillus ferrooxidans*

### 1 Introduction

The dissolution of copper sulfide minerals requires an oxidizing agent, and appropriate concentrations of ferric iron are usually used for this purpose [1]. High concentrations of ferric iron cause different forms of precipitates on the surface of ore particles, and, as a result, the accessibility of the leaching agent and the cells of the bacteria to the surfaces of the minerals decrease [2]. Ferrous iron is oxidized in acidic solutions by chemical and biological reactions; the biological oxidation of iron is faster than chemical oxidation [3]. Oxidation of ferrous iron in the bio-leaching process causes precipitates that usually contain schwertmannite ( $\text{Fe}_8\text{O}_8(\text{OH})_6\text{SO}_4$ ), ferrihydrite ( $5\text{Fe}_2\text{O}_3 \cdot 9\text{H}_2\text{O}$ ), and various types of jarosite ( $(\text{K}, \text{Na}, \text{NH}_4, \text{H}_2\text{O})\text{-Fe}_3(\text{SO}_4)_2(\text{OH})_6$ ) minerals [4].

Jarosite is a subgroup of alunite–jarosite minerals with general formula of  $\text{M}_n(\text{Fe}^{3+})_6(\text{SO}_4)_4(\text{OH})_{12}$ , where M can be K,  $\text{NH}_4$ , Na, Ag, or Pb, and  $n$  is two and one

for monovalent and divalent cations, respectively [5]. Some of the heavy elements replace potassium in the lattice of the jarosite crystals and, as a result, jarosite acts as a trap for the elements [6,7]. Formation of jarosite in the bio-leaching process requires cations, which can be acquired from the salts used as nutrients in the growth medium of bacteria; from the dissolution of minerals, such as mica, which loses its middle-layer potassium; and from acid-neutralizing additives, such as NaOH, KOH, and  $\text{K}_2\text{CO}_3$  [8]. The concentrations of the  $\text{NH}_4^+$ ,  $\text{K}^+$ , and  $\text{Na}^+$  cations determine the type of jarosite that is formed. The formation of potassium jarosite requires low concentrations of the aforementioned cations, whereas high concentrations are required for the formation of sodium jarosite. Generally, schwertmannite forms when there is a low concentration of monovalent cations in the aqueous phase [4]. The formation of jarosite increases in the presence of iron-oxidizing bacteria. LIU et al [9] reported that jarosite formation in the 9K medium began when *Acidithiobacillus ferrooxidans* bacteria underwent their logarithmic growth phase. It was reported that

bacteria's extracellular polymers affected the crystallization and uniformity of jarosite crystals. Jarosite that is formed in a biological environment is smaller in size, more intensive, and has a smoother surface than chemically-formed jarosite. The precipitate that is formed in the 9K medium usually contains potassium jarosite or a mixture of potassium and ammonium jarosite [10]. QIU et al [11] reported that chalcopyrite bio-leaching using a mixture of bacteria prevented the accumulation of jarosite on the surfaces of the minerals. GRAMP et al [4] showed that the solubility of  $\text{Fe}^{3+}$  was a function of pH in the leaching environment and that it had low solubility at pH values greater than 2. By examining the formation of jarosite in the 9K medium with pH values ranging from 1 to 3, DAOUD and KARAMANEV [12] showed that the lowest amount of jarosite formed occurred when the pH values were in the range of 1.6–1.7. CORDOBA et al [13] reported that ferrous ions had an important role in controlling of the creation of jarosite nuclei and the formation of precipitate. ZHU et al [14] found that the presence of ferrous ions in solution balanced the ferric iron concentration and prevented the formation of nuclei as well as the formation of precipitate on the surfaces of minerals. BIGHAM et al [8] investigated the effect of the temperature range from 2 to 40 °C on the chemical formation of jarosite and found that the precipitation rate increased as temperature increased. WANG et al [15] reported that when the temperature increased from 36 °C to 45 °C in a biological environment, schwertmannite was substituted with ammonium/hydronium jarosite. This substitution requires monovalent ions, and increases in the temperature facilitate the process.

As mentioned above, there are numerous variables that affect the production of ferric precipitate. These variables were usually examined in the absence of minerals, such as copper sulfides. The purpose of the present work is to examine the influence of the concentration of ferrous ions, pH and temperature on the

precipitation of ferric salts in a pulp that contains copper sulfide ore. To the knowledge of the authors, this is the first study that has addressed the effect of the formation of ferric precipitate on the ions that are necessary for *A. ferrooxidans* bacteria, such as ferrous, sulfate, magnesium, phosphate and potassium ions.

## 2 Experimental

### 2.1 Microorganism

In this study, a pure culture of *A. ferrooxidans* bacteria was used. The bacteria were separated from acid mine drainage from the Sarcheshmeh copper mine and adapted with low-grade Sarcheshmeh copper sulfide ore [16]. The growth medium (Table 1) with an initial pH of 1.8 was used for the *A. ferrooxidans* bacteria, and the medium containing the bacteria was placed in an incubator shaker with a shaking rate of 130 r/min and a temperature of 32 °C; 75 g of ferrous sulfate hydrate ( $\text{FeSO}_4 \cdot 7\text{H}_2\text{O}$ ) was used as the energy source [17–21]. After being incubated for 7 d, a culture of the bacteria that contained  $1.96 \times 10^8 \text{ mL}^{-1}$  was used in the experiments.

### 2.2 Sample of copper ore

The sample was prepared from a crushed ore stockpile that was used to feed a pilot-scale heap bio-leaching process in the Sarcheshmeh copper complex. The chemical and mineralogical compositions of the sample are reported in Tables 2 and 3. The results show that there were negligible amounts of copper oxides in the sample and that the vast majority of the copper minerals were in the form of primary sulfides (i.e., chalcopyrite).

The iron content of the sample was 7.3%, which is typical for minerals such as pyrite, chalcopyrite, hematite, and magnetite. The X-ray fluorescence (XRF) results (Table 3) indicated that the sample contained mainly silicate and alumina components; potassium and

**Table 1** Composition of growth medium [17]

Salt	$(\text{NH}_4)_2\text{SO}_4$	$\text{MgSO}_4 \cdot 7\text{H}_2\text{O}$	$\text{K}_2\text{HPO}_4$	KCl	$\text{Ca}(\text{NO}_3)_2 \cdot \text{H}_2\text{O}$
Dosage/(g·L <sup>-1</sup> )	3	0.5	0.63	0.1	0.014

**Table 2** Major sulfide minerals of ore sample (mass fraction)

Mineral	Chalcopyrite	Chalcocite	Covellite	Pyrite	Sphalerite	Molybdenite
Chemical formula	$\text{CuFeS}_2$	$\text{Cu}_2\text{S}$	$\text{CuS}$	$\text{FeS}_2$	$\text{ZnS}$	$\text{MoS}_2$
Quantity/%	1.86	0.05	0.02	13.88	0.11	0.04

**Table 3** XRF and chemical analyses of ore sample (mass fraction)

Oxide/element	$\text{Al}_2\text{O}_3$	$\text{SiO}_2$	CaO	$\text{K}_2\text{O}$	MgO	$\text{TiO}_2$	CuO	Cu	Fe	$\text{Fe}^{2+}$	$\text{Fe}^{3+}$
Assay/%	17.40	52.95	0.69	4.42	4.32	0.94	Trace	0.7	7.31	4.21	3.1

magnesium oxides were significant as well.

The X-ray diffraction (XRD) analysis (Fig. 1) showed that quartz ( $\text{SiO}_2$ ), chlorite ( $(\text{Mg,Fe})_6(\text{Si,Al})_4\text{O}_{10}(\text{OH})_8$ ), illite ( $(\text{K,H}_3\text{O})\text{Al}_2\text{Si}_3\text{AlO}_{10}(\text{OH})_2$ ), pyrite ( $\text{FeS}_2$ ), albite ( $(\text{Na,Ca})(\text{Al,Si})_4\text{O}_8$ ), muscovite ( $(\text{K,NH}_4,\text{Na})\text{Al}_2(\text{Si,Al})_4\text{O}_{10}(\text{OH})_2$ ) and chalcocopyrite ( $\text{CuFeS}_2$ ) are the main mineral constituents in the sample.

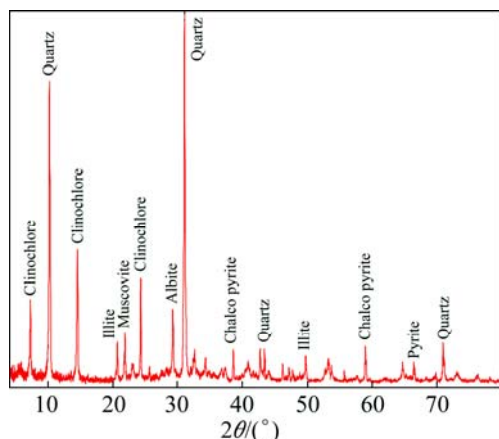


Fig. 1 XRD pattern of ore sample

### 2.3 Bio-leaching experiments

Bio-leaching experiments were performed in a 500-mL Erlenmeyer flask. The ore sample was ground to  $d_{80} < 108 \mu\text{m}$  and used in the experiments without sterilization. 200 mL of growth medium that had been inoculated by 10% (v/v) of a 7 d culture of *A. ferrooxidans* bacteria were used in the experiments. The solid fraction of 10% (w/w), leaching time of 11 d, shaking rate of 130 r/min, and a pre-determined dosage of ferrous sulfate ( $\text{FeSO}_4 \cdot 7\text{H}_2\text{O}$ ) as the source of ferrous iron were used in the experiments [3,11,22,23]. Sulfuric acid and sodium hydroxide solutions were used to adjust pH value to the desired values. The  $\phi_h$  and pH values were recorded daily. The final product of the bio-leaching process was filtered and washed with diluted sulfuric acid (5%) and hot, distilled water to remove any remaining medium and dissolved ions. The solid product was dried and analyzed for pre-determined elements or oxides. We had two main goals in this investigation:

1) The effects of pH, temperature, and the concentration of ferrous iron were evaluated on the deposition of ferric sulfate on the surfaces of the copper minerals. The conditions used were ferrous sulfate concentrations of 10 and 50 g/L, temperatures of 32 and 37 °C, and initial pH values of 1, 1.3, 1.6, 1.9, 2.2, and 2.5. The purpose was to determine the conditions that allow the production of the maximum amount of ferric precipitate.

2) The effects of the precipitation of ferric iron were determined on the availability of nutrient ions for the *A.*

*ferrooxidans* bacteria. During the bio-leaching process, the aqueous phase was sampled every 3 d to measure the concentrations of sulfate, phosphate, potassium, magnesium, total iron and ferrous iron.

Chemical analyses of the residues and solutions were performed by atomic absorption spectroscopy; scanning electron microscopy (SEM) and XRD measurements were used to characterize the precipitates.

## 3 Results and discussion

### 3.1 Efficiencies of oxidation of ferrous iron and production of ferric iron

BARRON and LUECKING [20] reported that the growth rate of *A. ferrooxidans* bacteria and the ability of the bacteria to oxidize ferrous iron were related to the concentration of ferrous iron in the aqueous phase. Ferrous iron is oxidized by *A. ferrooxidans* bacteria according to Eq. (1) [11]:



In this work, the ferrous iron oxidation efficiency and the amount of ferric iron produced were calculated according to Eqs. (2) and (3) [23]:

$$\eta = [\rho(\text{Fe}_{\text{in}}^{2+}) - \rho(\text{Fe}_{\text{out}}^{2+})] / \rho(\text{Fe}_{\text{in}}^{2+}) \times 100\% \quad (2)$$

$$\rho_1 = \rho(\text{Fe}_{\text{in}}^{2+}) - \rho(\text{Fe}_{\text{out}}^{2+}) \quad (3)$$

where  $\eta$  is the ferrous iron oxidation efficiency;  $\rho(\text{Fe}_{\text{in}}^{2+})$  and  $\rho(\text{Fe}_{\text{out}}^{2+})$  are the initial and final concentrations of ferrous iron in the aqueous phase, respectively;  $\rho_1$  is the ferric iron production.

Figures 2 and 3 show the efficiency of the oxidation of ferrous iron and the production rate of ferric iron, respectively, as functions of pH, temperature, and initial concentration of ferrous sulfate in the aqueous phase. Figures 2 and 3 show that, at pH values of 1.6 or greater, the efficiency of the oxidation of ferrous iron and the quantity of ferric iron produced for growth medium with a ferrous sulfate concentration of 50 g/L were greater than they were in the medium that had ferrous sulfate concentration of 10 g/L at both temperatures of 32 and 37 °C. In the former, the energy source for the microorganisms was greater than latter. At pH values greater than 1.6 (at the ferrous iron concentration of 50 g/L) and greater than 1.9 (at the ferrous iron concentration of 10 g/L), the iron oxidation efficiency and the ferric iron production at 32 °C exceeded those at 37 °C. Thus, the temperature of 32 °C was more suitable for the *A. ferrooxidans* bacteria [17], so both the ferrous iron oxidation rate and the ferric iron production were better at this temperature than at 37 °C. It also can be concluded that, for pH values less than 1.6, iron oxidation efficiency and ferric iron production at 37 °C were greater than those at 32 °C; in this case, chemical

oxidation was more effective than biological oxidation. For pH values greater than 1.6 (at the ferrous iron concentration of 50 g/L) and greater than 1.9 (at the ferrous iron concentration of 10 g/L), and at a temperature of 32 °C, the activity of the bacteria was the determining variable, and biooxidation was the predominant mechanism.

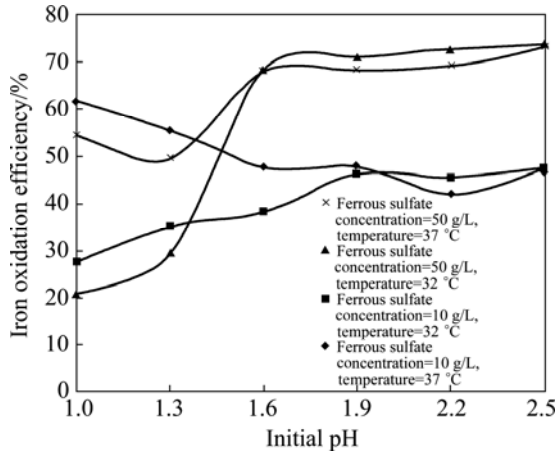


Fig. 2 Iron oxidation efficiency at different pH values, temperatures and ferrous iron concentrations

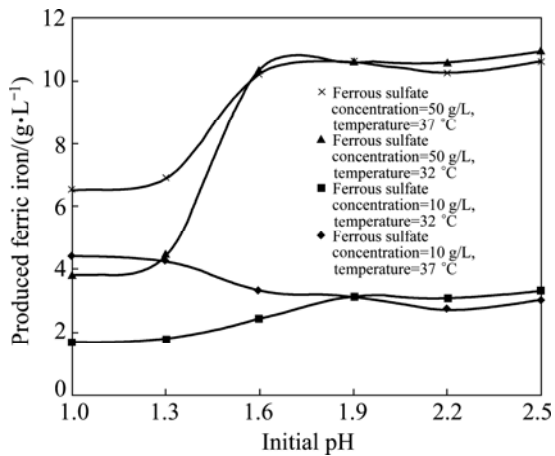


Fig. 3 Ferric iron production at different pH values, temperatures and ferrous iron concentrations

### 3.2 Precipitation of ferric iron

The ferric iron that was produced in the aqueous phase (Eq. (1)) can be hydrolyzed to ferric iron hydroxide (Eq. (4)), after which it combines with sulfate to produce iron sulfate hydroxide (Eq. (5)). In the presence of the required cations, iron sulfate hydroxide is converted to jarosite (Eq. (6)) [2,24–27]:

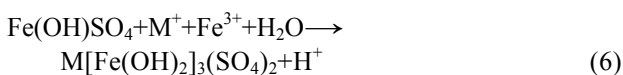


Figure 4 shows the amount of ferric iron that was precipitated as a function of pH, temperature, and the

initial concentration of ferrous sulfate in the aqueous phase. The amount of ferric iron that was precipitated was calculated according to the following equation [23]:

$$\rho_2 = \rho(\text{Fe}_{\text{tot},\text{in}}) - \rho(\text{Fe}_{\text{tot},\text{out}}) \quad (7)$$

where  $\rho(\text{Fe}_{\text{tot},\text{in}})$  and  $\rho(\text{Fe}_{\text{tot},\text{out}})$  are the initial and final concentrations (g/L) of total iron in the aqueous phase, respectively;  $\rho_2$  is the ferric iron precipitation.

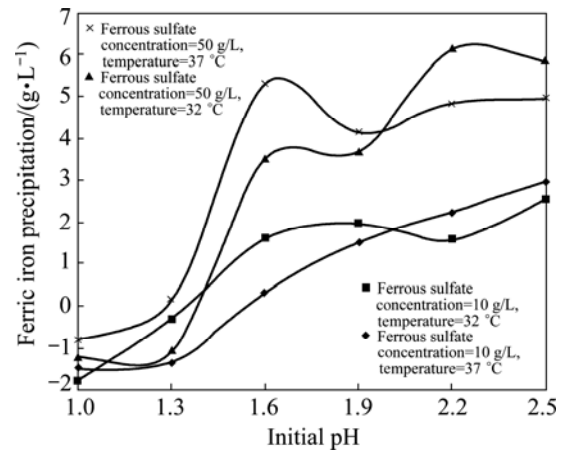


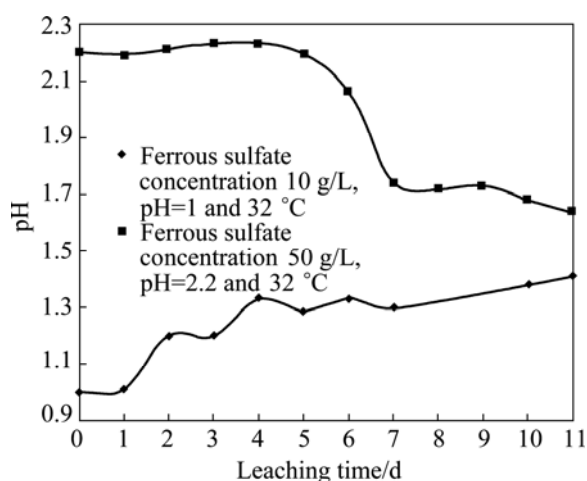
Fig. 4 Ferric iron precipitation at different pH values, temperatures and ferrous iron concentrations

GRAMP et al [4] reported that the solubility of ferric iron was a function of the pH of the aqueous phase, and the precipitation of ferric iron increased at the elevated pH values. Figure 4 shows that the precipitation of ferric iron begins at pH values of about 1.3, 1.35, 1.4, and 1.55 for aqueous phases with 50, 10, 50, and 10 g/L concentrations of ferrous sulfate at temperatures of 37, 37, 32, and 32 °C, respectively. For the elevated pH values, the overall trends for all four curves are upward. Figure 4 shows that, for all conditions that were examined when the pH was less than 1.3, the concentration of ferric iron in the solution increased as a result of the dissolution of the ferric iron in the ore, also preventing effect of the acidic condition on the precipitation of ferric iron; therefore, more ferric iron remained in solution at low pH values than at high pH values. It also can be concluded that the precipitation of ferric iron in solutions with ferrous sulfate at a concentration of 50 g/L and at pH values greater than 1.3 was greater than that in solutions with ferrous sulfate concentrations of 10 g/L at both 32 and 37 °C. The maximum precipitation of ferric sulfate was observed in the growth medium when the concentration of ferrous sulfate was 50 g/L at a temperature of 32 °C and an initial pH value of 2.2 (Fig. 4).

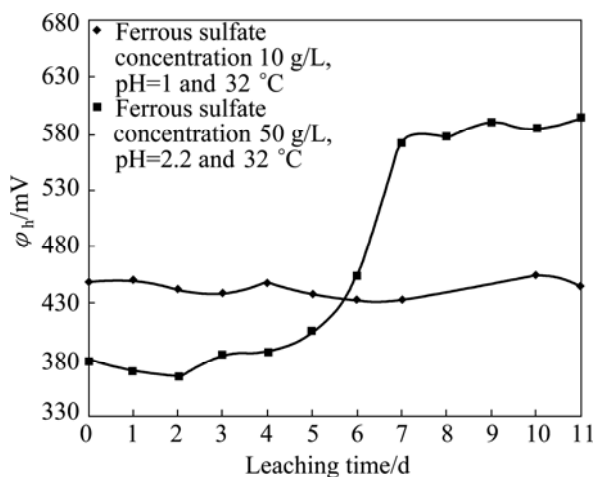
### 3.3 Variations of pH and $\phi_h$

Figure 5 shows the variations of pH as a function of leaching time for two different operating conditions: 1) a

ferrous sulfate concentration of 50 g/L, temperature of 32 °C, and initial pH of 2.2 and 2) a ferrous sulfate concentration of 10 g/L, temperature of 32 °C, and initial pH of 1. Figure 5 shows that, for condition 1, the pH value did not change significantly in 5 d; after that, it decreased as the leaching time increased. According to Eq. (4), the hydrolysis of ferric iron produces  $H^+$ , so the reduction on pH can be expected. In the first 5 d, the acid that was produced probably was consumed by the carbonate gangue minerals. In condition 2, an overall upward trend occurred as the leaching time increased; in this case, the hydrolysis and the subsequent acidification of the environment of the pulp were negligible, and the rate of acid consumption by the carbonate gangue minerals exceeded the rate of acid production. Figure 6 shows the variation of  $\varphi_h$  as a function of bio-leaching time for conditions 1 and 2. For condition 1, the ratio of  $Fe^{3+}/Fe^{2+}$  increased and, consequently,  $\varphi_h$  increased as the bio-leaching time increased. As mentioned in Fig. 5 and shown in Fig. 6, the activity of the bacteria increased



**Fig. 5** Effect of bio-leaching time on final pH of bio-leaching environment



**Fig. 6** Effect of bio-leaching time on final  $\varphi_h$  of bio-leaching environment

and the production of ferric iron increased as the bio-leaching time reached 6 d and beyond, and the pH was decreased to the desired range of 1.6–1.9 (Figs. 5 and 6). In the first 2 d of the test, the bacteria were in the lag phase, and the  $\varphi_h$  of the solution decreased slightly. After 2 d, the microorganisms entered the logarithmic growth phase, and the  $\varphi_h$  of solution increased; in the final 4 d of the test, the bacteria were in a stationary phase, and the  $\varphi_h$  values remained relatively constant.

For condition 2, the  $\varphi_h$  variations were not significant; thus, it can be concluded that the bacteria were at a low level of activity and that there was a low production of ferric iron.

### 3.4 Characterization of precipitate

Polarized light microscopy, SEM and XRD analyses were used to characterize the precipitate. Figure 7 shows a SEM image of a sample of the bio-leaching residue at condition 1 (section 3.3). As presented, jarosite coated some parts of the surfaces of the particles of ore, which contained sulfide minerals. An elemental analysis of the surfaces assigned to jarosite is shown in Fig. 8; iron, potassium, sulfur, silicon, aluminum, and magnesium were identified, some of which were found in the jarosite mineral and some of which resulted from the inclusion of the mineral matter. The precipitation of jarosite on the surface of the bio-leaching residue in the condition 1 also was evident in the polarized light microscopy photograph in Fig. 9. Figure 10 shows the XRD analysis of the sample of bio-leaching residue at condition 1. We were able to identify quartz ( $SiO_2$ ), chlorite ( $(Mg,Fe)_6(Si,Al)_4O_{10}(OH)_8$ ), muscovite ( $(K,NH_4,Na)Al_2(Si,Al)_4O_{10}(OH)_2$ ), albite ( $(Na,Ca)(Al,Si)_4O_8$ ), jarosite ( $KFe_3(SO_4)_2(OH)_6$ ), illite ( $(K,H_3O)Al_2Si_3AlO_{10}(OH)_2$ ), azurite ( $2CuCO_3 \cdot Cu(OH)_2$ ), and pyrite ( $FeS_2$ ). Based on XRD and SEM analyses, the precipitate was mainly from the jarosite group.

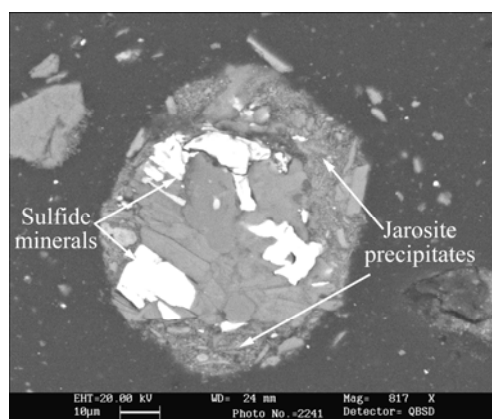


**Fig. 7** SEM image of bioleaching residue (ferrous sulfate concentration 50 g/L, temperature 32 °C, initial pH 2.2, bio-leaching time 11 d)

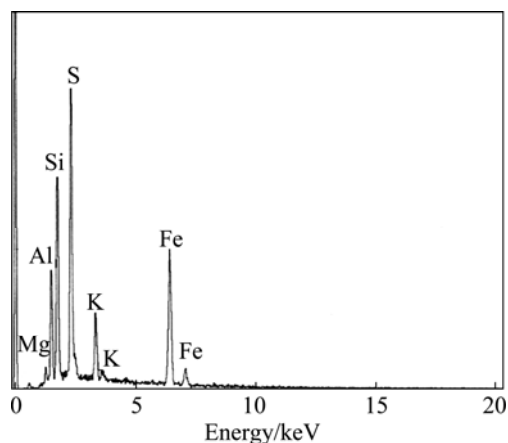


Fig. 8 Elemental analysis of jarosite precipitate in Fig. 7



Fig. 9 Polarized light photomicrograph of bio-leaching residue (ferrous sulfate concentration 50 g/L, temperature 32 °C, initial pH 2.2, bio-leaching time 11 d)

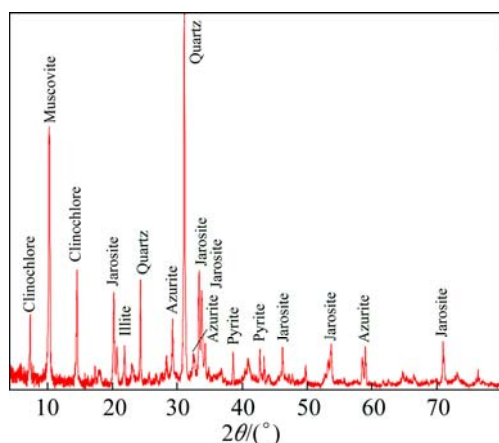


Fig. 10 XRD pattern of bio-leaching residue (ferrous sulfate concentration 50 g/L, temperature 32 °C, initial pH 2.2, bioleaching time 11 d)

### 3.5 Effect of precipitation of ferric iron on ions that are important for *A. ferrooxidans* bacteria

In the following sections, we assessed the effects of the precipitation of ferric iron on the levels of soluble ferric, sulfate, magnesium, potassium, and phosphate ions in the aqueous phase of the bio-leaching

environment. In the experiments, we considered different pH values of 1, 1.3, 1.6, 1.9, 2.2, and 2.5, a temperature of 32 °C, and an initial ferrous sulfate concentration of 50 g/L.

#### 3.5.1 Variation of ferric iron concentration

Figure 11 shows the soluble ferric iron in the aqueous phase (g/L) at various pH values and leaching times. For all of the pH values that were used, an increase of soluble ferric iron was observed in the first few days of the bio-leaching process. The maximum ferric iron concentrations for pH values of 2.5, 2.2, 1.9, 1.6, 1.3, and 1, were observed at leaching time of 2, 3, 4, 5, 3, and 5 d, respectively; thereafter, as the leaching time increased, reductions of the soluble ferric iron were observed. In the first few days of the bio-leaching process, the oxidation of ferrous sulfate and the dissolution of ferric iron from the ore sample increased the soluble ferric iron. After the maximum values were reached, the precipitation of the ferric iron led to a decreased concentration of soluble ferric iron in the solution. High levels of precipitation (low levels of soluble ferric iron) were observed for pH values greater than 1.6 after 5 d of bio-leaching.

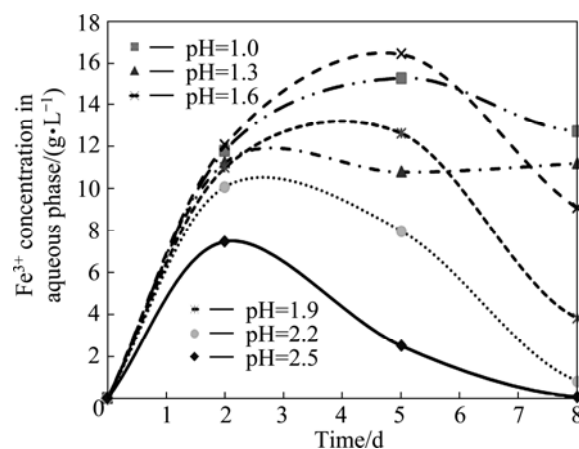


Fig. 11 Variations of soluble ferric iron in aqueous phase

#### 3.5.2 Variation of sulfate concentration

Figure 12 shows the sulfate levels in the solution different pH values and leaching times. For pH values of 1.6 and lower, increase in soluble sulfate was observed as leaching time increased; this could result from the oxidation of sulfide-containing minerals and also from the low level of precipitation of ferric sulfate in this range of pH values. For pH values of 1.9 and greater, different patterns were observed as leaching time increased; the performance can be changed depending on the positive effect of the oxidation of sulfide minerals (to produce sulfate ions) and on the negative effect of the precipitation of ferric sulfate (which reduces the sulfate concentration in the solution).

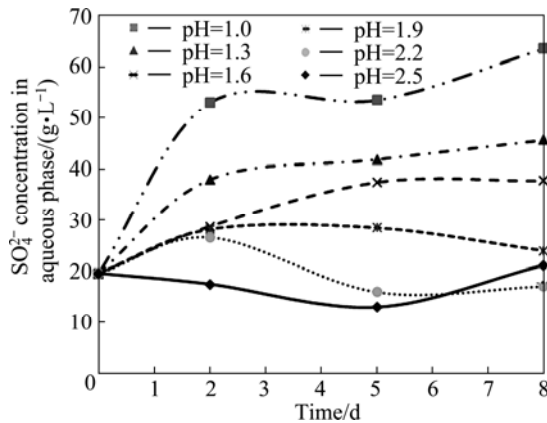


Fig. 12 Variations of soluble  $\text{SO}_4^{2-}$  ions in aqueous phase

### 3.5.3 Variation of potassium concentration

Figure 13 shows potassium concentrations in the aqueous phase as a function of pH and leaching time. In the first few days of leaching, it was observed that the  $\text{K}^+$  concentration increased for all of the pH values that were assessed; this may be due to the dissolution of a gangue constituent in the ore; thereafter, the  $\text{K}^+$  concentration decreased. High levels of reduction were observed for pH values greater than 1.9. Again, the high level of potassium-jarosite precipitation could be the reason.

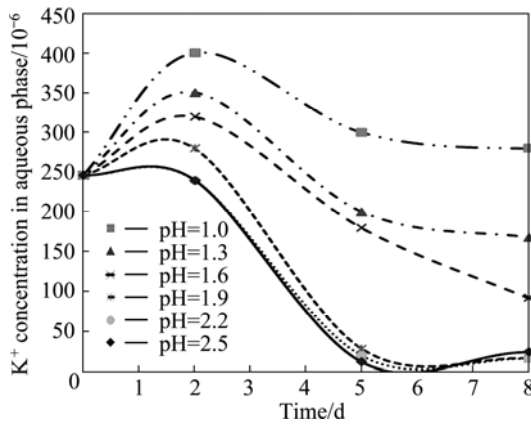


Fig. 13 Variations of soluble  $\text{K}^+$  ions in aqueous phase

A relatively common pattern was observed for the ferric, sulfate, and potassium ions at the extended leaching time, and this was due to their co-precipitation as constituents of jarosite (Eqs. (4)–(6)).

### 3.5.4 Variation of phosphate concentration

Figure 14 shows the variation of soluble phosphate as a function of pH and bio-leaching time. While the pH values were 1 and 1.3, no significant reduction of soluble phosphate was observed due to the low activity of the bacteria and low ferric precipitation; however, when the pH values were 1.6 and greater, rapid reduction on phosphate levels was observed due to the co-precipitation of phosphate with ferric sulfate and the high activity of bacteria.

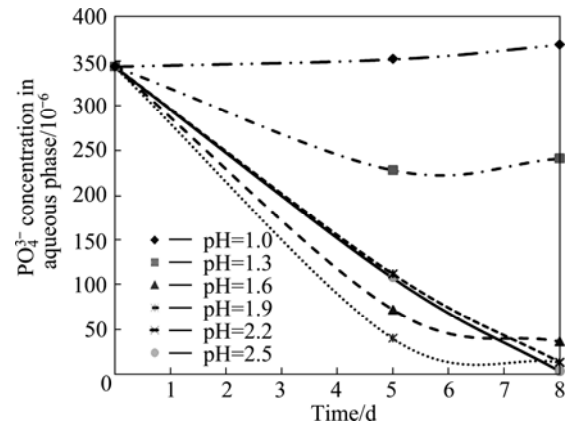


Fig. 14 Variations of soluble  $\text{PO}_4^{3-}$  ions in aqueous phase

### 3.5.5 Variation of magnesium concentration

Figure 15 shows the variations of soluble magnesium in solution for different leaching times and pH values. For all of the pH values that were used, the magnesium levels increased in the first few days of the bio-leaching process. Dissolution of a gangue constituent in the ore may be a reason; thereafter, the  $\text{Mg}^{2+}$  concentrations decreased slightly. Low levels of  $\text{Mg}^{2+}$  concentrations were observed for pH values greater than 1.9. Again, the co-precipitation of magnesium with jarosite mineral and the high activity of the *A. ferrooxidans* bacteria can cause a reduction in soluble magnesium ions.

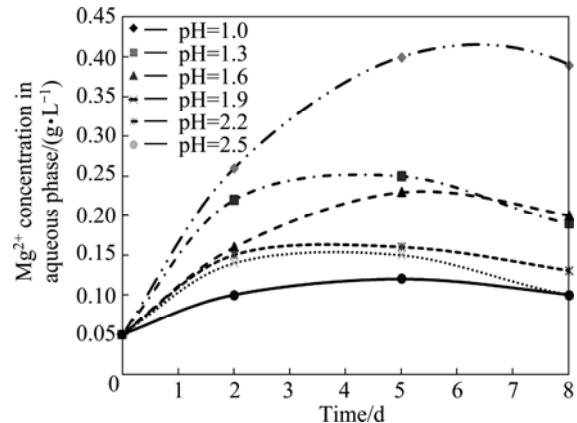


Fig. 15 Variations of soluble  $\text{Mg}^{2+}$  ions in aqueous phase

## 4 Conclusions

1) Under the conditions of a ferrous sulfate concentration of 50 g/L, a temperature of 32 °C, and an initial pH value of 2.2, the maximum quantity of ferric iron was precipitated. Decreasing pH, increasing temperature, or decreasing the concentration of ferrous sulfate from the above-mentioned values resulted in decreases in the precipitation of ferric iron.

2) Low levels of soluble ferric iron were observed for pH values greater than 1.9 after 5 d of the

bio-leaching process.

3) At the examined pH values of 1.9, 2.2, and 2.5, different patterns for the soluble sulfate ions were observed as leaching time increased. This behavior can be dictated by the positive effect of the oxidation of the sulfide minerals or the negative effect of the precipitation of ferric sulfate.

4)  $K^+$  concentration was reduced significantly after 5 d of the bio-leaching process at pH levels greater than 1.9. This likely was due to the large amounts of potassium-jarosite that were precipitated.

5) At pH values greater than 1.6, the solubility of phosphate ions decreased significantly; the likely cause was the co-precipitation of phosphate with jarosite and the high level of activity of the *A. ferrooxidans* bacteria at these pH values.

6) For all the examined pH values, the dissolution of a gangue constituent in the ore increased the magnesium levels in the first few days of the bio-leaching process; after that, the  $Mg^{2+}$  concentrations decreased slightly.

## Acknowledgment

The authors gratefully acknowledge the financial support provided by the R&D division of the Sarcheshmeh Copper Complex and Tehran Science and Research Branch at Islamic Azad University.

## References

- [1] WATLING H R. The bioleaching of sulfide minerals with emphasis on copper sulfides—A review [J]. *Hydrometallurgy*, 2006, 84: 81–108.
- [2] CORDOBA E M, MUNOZ J A, BLAZQUEZ M L, GONZALEZ F, BALLESTER A. Leaching of chalcopyrite with ferric ion. Part I: General aspects [J]. *Hydrometallurgy*, 2008, 93: 81–87.
- [3] OZKAYA B, SAHINKAYA E, NURMI P, KAKSONEN A H, PUHAKKA J A. Iron oxidation and precipitation in simulated heap leaching solution in a *Leptospirillum ferriphilum* dominated biofilm reactor [J]. *Hydrometallurgy*, 2007, 88: 67–74.
- [4] GRAMP J P S, JONES F S, BIGHAM J M, TUOVINEN O H. Monovalent cation concentrations determine the types of Fe(III) hydroxyl sulfate precipitates formed in bioleach solutions [J]. *Hydrometallurgy*, 2008, 94: 29–33.
- [5] BASCIANO L C. Crystal chemistry of the jarosite group of minerals: Solid-solution and atomic structures [D]. Kingston, Ontario, Canada: Department of Geological Sciences and Geological Engineering, Queen's University, 2008, Section 1: 1–9.
- [6] DUTRIZAC J E, HARDY D J, CHEN T T. The behaviour of cadmium during jarosite precipitation [J]. *Hydrometallurgy*, 1996, 41(2–3): 269–285.
- [7] SMITH A H, KAREN D W, WRIGTH K. Defects and impurities in jarosite: A computer simulation study [J]. *Applied Geochemistry*, 2006, 21(8): 1251–1258.
- [8] BIGHAM J M, JONES F S, OZKAYA B, SAHINKAYA E, PUHAKKA J A, TUOVINEN O H. Characterization of jarosite produced by chemical synthesis over a temperature gradient from 2 to 40 °C [J]. *International Journal of Mineral Processing*, 2010, 94: 121–128.
- [9] LIU J, LI B, ZHONG D, XIA L, QIU G. Preparation of jarosite by *A. ferrooxidans* oxidation [J]. *Journal of Central South University of Technology*, 2007, 14(5): 623–628.
- [10] SASAKI K, KONNO H. Morphology of jarosite-group compounds precipitated from biologically and chemically oxidized Fe ion [J]. *The Canadian Mineralogist*, 2000, 38: 45–66.
- [11] QIU M, XIONG S, ZHANG W, WANG G. A comparison of bioleaching of chalcopyrite using pure culture or a mixed culture [J]. *Minerals Engineering*, 2005, 18: 987–990.
- [12] DAOUD J, KARAMANEV D. Formation of jarosite during  $Fe^{2+}$  oxidation by *Acidithiobacillus ferrooxidans* [J]. *Minerals Engineering*, 2006, 19: 960–967.
- [13] CORDOBA E M, MUNOZ J A, BLAZQUEZ M L, GONZALEZ F, BALLESTER A. Leaching of chalcopyrite with ferric ion. Part II: Effect of redox potential [J]. *Hydrometallurgy*, 2008, 93: 88–96.
- [14] ZHU I, WU C, LU W, LIU Y, MA Y, CHEN A. Jarosite-related chemical processes and water ecotoxicity in simplified anaerobic microcosm wetlands [J]. *Environmental Geology*, 2008, 53: 1491–1502.
- [15] WANG H, BIGHAM J M, TUOVINEN O H. Formation of schwertmannite and its transformation to jarosite in the presence of acidophilic iron-oxidizing microorganisms [J]. *Materials Science and Engineering C*, 2006, 26: 588–592.
- [16] SEYYEDBAGHERI S A, HASSANI H R. Isolation and preliminary identification of some iron-and sulfur-oxidizing microorganisms from the Sarcheshmeh copper mine [C]//CIMINELLI S T, GARCIA O Jr. *Biohydrometallurgy: Fundamentals, Technology and Sustainable Development. Part A, Bioleaching, Microbiology and Molecular Biology*. Amsterdam: Elsevier, 2001: 393–396.
- [17] NEMATI M, HARRISON S T L, HANSFORD G S, WEBB C. Biological oxidation of ferrous sulfate by *Thiobacillus ferrooxidans*: A review on the kinetic aspects [J]. *Biochemical Engineering*, 1998: 171–190.
- [18] LACEY D T, LAWSON F. Kinetics of the liquid-phase oxidation of acid ferrous sulfate by the bacteria *Thiobacillus ferrooxidans* [J]. *Biotechnology and Bioengineering*, 1970, 12: 29–50.
- [19] KARAMANEV D G. Model of the biofilm structure of *Thiobacillus ferrooxidans* [J]. *Journal of Biotechnology*, 1991, 20(1): 51–64.
- [20] BARRON J L, LUECKING D R. Growth and maintenance of *Thiobacillus ferrooxidans* cell [J]. *Applied and Environmental Microbiology*, 1990, 56(9): 2801–2806.
- [21] JENSEN A, WEBB C. Ferrous sulfate oxidation using *Thiobacillus ferrooxidans*: A review [J]. *Process Biochemistry*, 1995, 30(3): 225–236.
- [22] ZAMANI M A, VAGHAR R, OLIAZADEH M. Selective copper dissolution during bioleaching of molybdenite concentrate [J]. *International Journal of Mineral Processing*, 2006, 81: 105–112.
- [23] NURMI P, OZKAYA B, KAKSONEN A H, TUOVINEN O H, RIEKKOLA-VANHANEN M L, PUHAKKA J A. Process for biological oxidation and control of dissolved iron in bioleach liquors [J]. *Process Biochemistry*, 2009, 44: 1315–1322.
- [24] SERGEI I G, BIGHAM J M, TUOVINEN O H. Characterization of jarosite formed upon bacterial oxidation of ferrous sulfate in a packed-bed reactor [J]. *Applied and Environmental Microbiology*, 1988, 54: 3101–3106.
- [25] JIANG H, LAWSON F. Reaction mechanism for the formation of ammonium jarosite [J]. *Hydrometallurgy*, 2006, 82: 195–198.
- [26] YIN S H, WU A X, QIU G Z. Bioleaching of low-grade copper sulphides [J]. *Transactions of Nonferrous Metals Society of China*, 2008, 18(3): 707–713.
- [27] DING J N, GAO J, WU X L, ZHANG C G, WANG D Z, QIU G Z. Jarosite-type precipitates mediated by YN22, *Sulfobacillus thermosulfidooxidans*, and their influences on strain [J]. *Transactions of Nonferrous Metals Society of China*, 2007, 17(5): 1038–1044.

## 黄钾铁矾的生成机理及其对嗜酸氧化亚铁硫杆菌有重要作用的离子的影响

B. NAZARI<sup>1</sup>, E. JORJANI<sup>1</sup>, H. HANI<sup>1</sup>, Z. MANAFI<sup>2</sup>, A. RIAHI<sup>2</sup>

1. Department of Mining Engineering, Tehran Science and Research Branch, Islamic Azad University, Tehran, Iran;

2. Hydrometallurgy Research Center, Sarcheshmeh Copper Complex,  
National Iranian Copper Industries Company, Iran

**摘要:** 黄钾铁矾的生成对 Sarcheshmeh 生物堆浸硫化铜矿有不利影响。实验研究了在嗜酸氧化亚铁硫杆菌存在的情况下, 生长介质中 Fe(II)的初始浓度、pH 及温度影响黄钾铁矾沉淀形成的机理。产生最多 Fe(III)沉淀的条件为: 硫酸亚铁浓度 50 g/L、初始 pH 2.2、温度 32 °C。Fe(III)沉淀的生成影响了对嗜酸氧化亚铁硫杆菌有重要作用的离子的浓度, 比如:  $\text{Fe}^{3+}$ 、 $\text{SO}_4^{2-}$ 、 $\text{K}^+$ 、 $\text{PO}_4^{3-}$ 、 $\text{Mg}^{2+}$ 。对于  $\text{Fe}^{3+}$ 和  $\text{K}^+$ , 他们有相似的模式, 这些离子共沉淀而形成黄钾铁矾的组分。在 pH 高于 1.6 时, 由于  $\text{PO}_4^{3-}$  与黄钾铁矾共沉淀以及嗜酸氧化亚铁硫杆菌较快的生长速度而导致含  $\text{PO}_4^{3-}$  的化合物的溶解度急剧降低。在生物堆浸的初期, 由于脉石的溶解,  $\text{Mg}^{2+}$  浓度增大, 随后缓慢降低。

**关键词:** 黄钾铁矾的生成; 生物浸铜; 嗜酸氧化亚铁硫杆菌

(Edited by Hua YANG)